https://dx.doi.org/10.1016/j.jcsr.2017.06.008


# Experimental Investigation into High Strength Q690 Steel Welded H-sections under Combined Compression and Bending

Tian-Yu Ma[1,2], Yi-Fei Hu[2], Xiao Liu[2,3], Guo-Qiang Li[1], Kwok-Fai Chung[2,3]

[1] *College of Civil Engineering, Tongji University, Shanghai, China*

[2] *Department of Civil and Environmental Engineering, the Hong Kong Polytechnic University, Hong Kong SAR, China*

[3] *Chinese National Engineering Research Centre for Steel Construction (Hong Kong Branch), Hong Kong SAR, China*

**Abstract:** This paper presents a systematic experimental investigation into high strength Q690 steel welded H-sections under combined compression and bending. A total of 8 slender columns with four sections of different cross-sectional dimensions were tested successfully under eccentric loads. All columns failed in overall buckling about the minor axes of their cross-sections with significant material yielding. In some cases, plastic local plate buckling in the flange outstands became apparent at failure. After tests, all the columns were inspected closely, and no fracture in welding was found. As expected, these high strength Q690 steel welded H-sections were demonstrated to behave in various ways similar to those of conventional strength steel welded H-sections. Hence, these tests may be regarded to be confirmatory tests to structural behavior of Q690 steel welded H-sections under combined compression and bending.

It should be noted that the measured failure loads were compared with the predicted resistances of these H-sections based on their measured geometrical and material properties according to various design rules given in EN1993-1-1, ANSI/AISC 360-16 and GB 50017-2003 respectively. Among all these three sets of design rules, EN1993-1-1 is shown to be effective and efficient in predicting resistances for high strength Q690 steel welded H-sections under combined compression and bending with properly selected parameters. Hence, EN1993-1-1 should be readily adopted by design and construction engineers in designing these Q690 steel welded H-sections under combined compression and bending.

**Keywords:** **High strength steel; Welded H-sections; Combined compression and bending; Experiment**

## 1 Introduction

Nowadays, "high strength steel" commonly refers to those steel materials with a yield strength equal to or higher than 690 N/mm$^2$, i.e. two to three times of conventional steel



© 2017. This manuscript version is made available under the CC-BY-NC-ND 4.0 license http://creativecommons.org/licenses/by-nc-nd/4.0/

materials with yield strengths of 235 and 345 N/mm$^2$. Compared with those conventional steel materials, high strength steel materials exhibit a limited degree of strain hardening after yielding, and a reduced ductility with a smaller elongation at fracture. Moreover, the values of tensile to yield strength ratios are also decreased. These differences in the mechanical properties of high strength steel materials may have significant effects on the structural behavior of steel sections made of high strength steel materials. In the past decade, high strength steel sections have been used in a number of projects [1] [2] [3] [4], and their economic benefits have been assessed [5] [6] to establish overall cost effectiveness in these structures.

Steel sections made of high strength steel materials are expected to behave in various ways, though not identical, similar to those of conventional steel materials. It is generally believed that differences in stress-strain curves, effects of welding and geometrical initial imperfections will have beneficial as well as non-beneficial effects on the structural behavior of steel sections made of high strength steel materials.

### 1.1 Testing of columns made of high strength steel materials

A number of experimental investigations have been conducted on high strength steel columns under axial compression. Rasmussen and Hancock [7] measured compressive resistances of welded sections made of 690 N/mm$^2$ steel and concluded that the limiting plate slendernesses for yielding obtained from sections made of conventional steel materials were also applicable to similar sections made of high strength steel materials. Yuan [8] compared deformation capacities of stocky columns made of different steel materials, and he found that those limiting values for section classification obtained from sections made up of conventional steel materials could not always guarantee sufficient deformation capacities when applied directly to high strength steel sections.

Moreover, Rasmussen and Hancock [9], Li et al. [10], and Ban et al. [11] examined flexural buckling resistances of various welded sections made of 690 and 960 N/mm$^2$ steel materials. All these H-sections were tested with buckling about minor axes of the cross-sections. It should be noted that a major test programme on high strength steel welded H-sections buckling about major axes of their cross-sections were conducted by Shi et al. [12]. In these tests, the section ends were restrained with beams while out-of-plane and torsional deformations were restrained with braces. All these specimens in the literature [9] [10] [11] [12] were found to buckle with axial resistances significantly higher than those predicted with codified design rules. These resistance enhancements were materialized because of the presence of reduced residual stresses and initial geometrical out-of-straightness as well as the presence of restraints in the sections. However, for those sections made of 460 N/mm$^2$ steel materials, their resistance enhancements in axial buckling resistance were found not to be as significant as those made of Q690 and Q960 steel materials [13] [14] [15] [16].

There were few reports on high strength steel Q690 sections under combined compression and bending. Usami et al. [17] studied the interaction between local and overall buckling of HT80 steel welded box sections under concentric and eccentric loads. The test results showed a good agreement with a proposed empirical design formula. Li et al [18] [19] tested a number of welded H-sections and box-sections made of Q460 high strength steel materials. All the measured resistances were found to be higher than predicted resistances using design rules given in the Chinese Steel Code GB 50017-2003. Yan et al [20] established a numerical model, and the model was demonstrated to be able to give good predictions to those test results given in [19].

### 1.2 Design rules applicable to slender columns made of high strength steel materials

Currently, there are a number of design methods whose scopes of applicability cover or may be readily expanded to cover steel sections made of high strength Q690 steel materials. The European Steel Code EN 1993-1-1 [21] provides a unified design method for flexural buckling of both rolled and welded sections made of S235 to S460 steel materials. To extend the design method to cover welded sections made of high strength steel materials, EN 1993-1-12 [22] gives supplementary rules for steel materials up to S700 in a simple and conservative manner. The American Steel Code ANSI/AISC 360-16 [23] also covers steel sections made of steel materials up to 690 N/mm$^2$ (ASTM A514 and A709 steel), and it does not differentiate high strength steel materials from conventional steel materials. On the contrary, the Chinese Steel Code GB 50017-2003 [24] is only applicable to Q235 to Q420 steel materials as both experimental evidence and theoretical background of all the design rules are based on the structural behavior of conventional steel materials. This shortcoming should be overcome in order to facilitate a wide adoption of steel sections made of Q690 steel materials in China.

### 1.3 Objectives and scope of work

In order to promote a wide application of high strength Q690 steel structures, it is necessary to investigate experimentally the structural behavior of Q690 steel welded H-sections and to identify or establish supplementary design rules through calibration against test results.

This paper presents a systematic experimental investigation into high strength Q690 steel welded H-sections under combined compression and bending. A total of 8 slender columns with four sections of different cross-sectional dimensions were tested successfully under eccentric loads. It should be noted that the experimental investigation was devised in such a way that the non-dimensional slendernesses of the columns ranged from 0.6 to 1.8, i.e. within the range of intermediate slenderness. These high strength Q690 steel welded H-sections are expected to behave in various ways similar to those of welded H-sections made of conventional steel materials. Hence, these tests may be regarded to be confirmatory tests to structural behavior of Q690 steel welded H-sections under combined compression and bending.

After testing, failure loads of these welded H-sections will be compared directly with predicted resistances of corresponding sections based on their measured geometrical and material properties according to various design rules given in European, American and Chinese Steel Codes. It aims to establish the applicability of these design rules for high strength Q690 steel welded H-sections under combined compression and bending through calibration against test results.

# 2 Experimental Investigation

## 2.1 Test Program

A total of 8 slender columns of welded H-sections were tested under eccentric loads, and hence, these columns were under combined compression and bending about the minor axes of the cross-sections of the H-sections. These columns were made from high strength Q690-QT steel plates with nominal thicknesses of 6, 10 and 16 mm. Four sections of different cross-sectional dimensions, namely, Sections H1, H2, H3 and H4 were involved. The nominal cross-sectional dimensions and their section classifications according to EN 1993-1-1 and ANSI/AISC 360-16 are shown in Figure 1 while the measured dimensions and section properties of these four welded H-sections are summarized in Table 1.

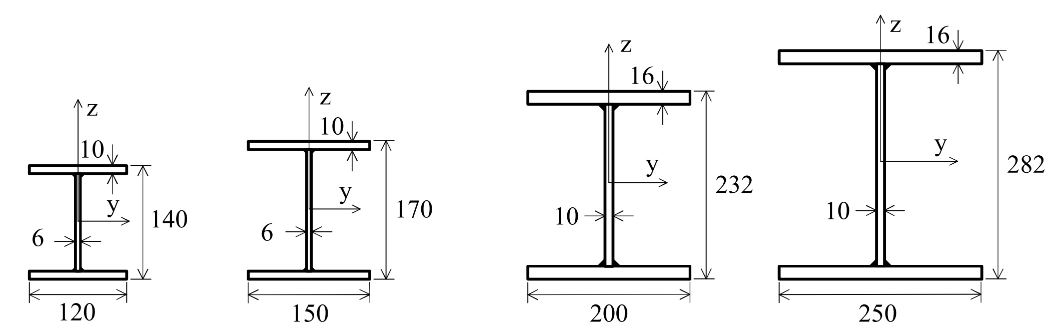


*Class 1* *Compact* a) Section H1 | *Class 3* *Non-compact* b) Section H2 | *Class 2* *Compact* c) Section H3 | *Class 3* *Non-compact* d) Section H4

**Figure 1 Nominal cross-sectional dimensions of welded H-sections**

**Table 1 Measured dimensions and section properties of welded H-sections**

| Test | Section depth $h$ (mm) | Section width $b$ (mm) | Flange thickness $t_f$ (mm) | Web thickness $t_w$ (mm) | Specimen length $L_s$ (mm) | Effective length $L_{eff}$ (mm) | Area $A$ ($mm^2$) | Second moment of area $I_z$ ( $\times 10^6$ $mm^4$) | Radius of gyration $i_z$ (mm) |
|---|---|---|---|---|---|---|---|---|---|
| EH1P | 140.0 | 119.6 | 9.90 | 5.83 | 1612 | 1992 | 3070 | 2.83 | 30.4 |
| EH1Q | 141.2 | 119.8 | 9.91 | 5.85 | 2410 | 2790 | 3085 | 2.84 | 30.3 |
| EH2P | 170.0 | 149.3 | 9.90 | 5.81 | 1613 | 1993 | 3827 | 5.49 | 37.9 |
| EH2Q | 170.0 | 149.7 | 9.92 | 5.85 | 2410 | 2790 | 3847 | 5.54 | 38.0 |
| EH3P | 231.8 | 201.5 | 15.98 | 9.92 | 1613 | 1993 | 8422 | 21.81 | 50.9 |
| EH3Q | 231.7 | 200.7 | 15.97 | 9.95 | 2412 | 2792 | 8397 | 21.54 | 50.6 |
| EH4P | 284.2 | 250.1 | 15.97 | 9.92 | 1611 | 1991 | 10490 | 41.66 | 63.0 |
| EH4Q | 282.0 | 249.9 | 15.93 | 9.93 | 2410 | 2790 | 10448 | 41.47 | 63.0 |

## 2.2 Fabrication of welded H-sections

All the steel plates were cut to size using a high power flame plasma cutting machine. Before welding, the steel plates were tack welded to form H-sections, and a pre-heating of 120 °C was applied to web-to-flange junctions to facilitate quality welding. For each section, the web was connected to the flanges with fillet welds on both sides of the web. Gas metal arc welding (GMAW) with a fillet size of 6 mm was used for Sections H1 and H2 while submerged arc welding (SAW) with a fillet size of 10 mm was used for Sections H3 and H4. The fillet sizes were assigned to be the same of the web thicknesses of the H-sections to ensure structural adequacy. Each fillet was formed in a single run which was staggered with a length of 500 to 600 mm along the column length to minimize distortion due to welding. Both material specifications of the welding electrodes and the welding parameters are shown in Table 2. As the electricity parameters fluctuated during welding, average values were taken. After the H-section was assembled, a pair of Q345 steel 30 mm thick plates were welded onto both ends of the H-section. Moreover, triangular stiffeners were welded at both ends to strengthen the connections locally between the endplates and the flanges of the H-section.

**Table 2 Technical information on welding**

| Section | Welding method | Material specification of welding electrodes | | | | Welding parameters | | | |
|---|---|---|---|---|---|---|---|---|---|
| | | Trade mark | Diameter (mm) | Yield strength (N/mm²) | Tensile strength (N/mm²) | Voltage (V) | Current (A) | Speed (mm/s) | Fillet size (mm) |
| H1 & H2 | GMAW | CHW-80C1 | 1.2 | 660 | 760 | 30 | 240 | 4.1 | 6 |
| H3 & H4 | SAW | CHW-S80 | 4.0 | 680 | 760 | 36 | 450 | 6.1 | 10 |

## 2.3 Mechanical Properties

In order to obtain the material properties of Q690 steel plates, a total of nine tensile tests were carried out in accordance with EN ISO 6892-1 [25]. The stress-strain curves for all the tensile tests are plotted in Figure 2. It is found that for all the Q690 steel plates with different thicknesses, no definite plateau after yielding is present, and strain hardening occurs shortly after yielding takes place. The measured material properties are summarized in Table 3.

It should be noted that EN 1993-1-12 specifies the following ductility criteria for steel materials with steel grades from S460 up to S700: i) $f_u$ / $f_y \geq 1.05$; ii) elongation at failure not less than 10 %; and iii) $\varepsilon_u \geq 15\ f_y$ / E. It is shown that all the steel plates satisfy these ductility criteria, and they are readily qualified to be high strength steel materials to EN 1993-1-12.

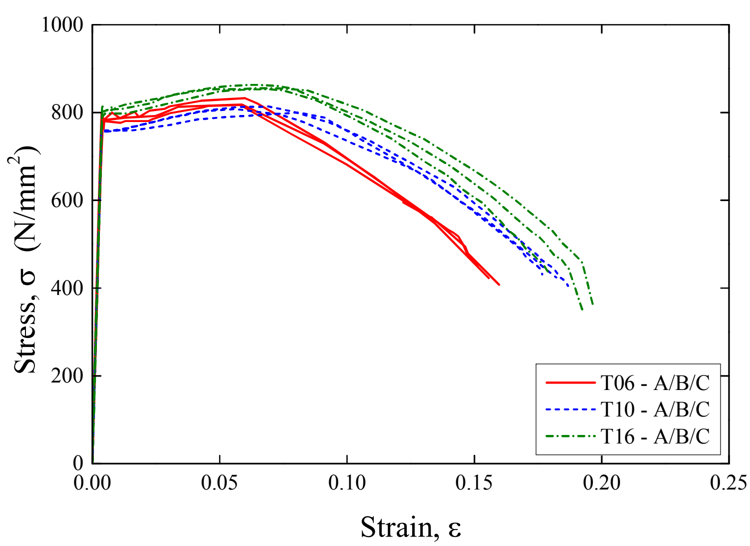


**Figure 2 Stress-strain curves of Q690 steel plates**

**Table 3 Mechanical properties of Q690 steel plates**

| Nominal thickness t (mm) | Coupon | Young's modulus E ($kN/mm^2$) | Yield strength $f_y$ ($N/mm^2$) | Tensile strength $f_u$ ($N/mm^2$) | Ratio $f_u/f_y$ | Strain at $f_u$ $\varepsilon_u$ | Elongation at fracture A (%) |
|---|---|---|---|---|---|---|---|
| 6 | T06-A | 210 | 771 | 819 | 1.06 | 0.059 | 15.5 |
| | T06-B | 210 | 764 | 810 | 1.06 | 0.060 | 15.3 |
| | T06-C | 209 | 763 | 817 | 1.07 | 0.058 | 16.0 |
| | Average | 210 | 766 | 815 | 1.06 | 0.059 | 15.6 |
| 10 | T10-A | 212 | 753 | 788 | 1.05 | 0.065 | 18.2 |
| | T10-B | 214 | 758 | 796 | 1.05 | 0.078 | 18.9 |
| | T10-C | 211 | 756 | 794 | 1.05 | 0.067 | 18.7 |
| | Average | 212 | 756 | 793 | 1.05 | 0.070 | 18.6 |
| 16 | T16-A | 208 | 800 | 855 | 1.07 | 0.064 | 19.7 |
| | T16-B | 206 | 797 | 833 | 1.05 | 0.065 | 17.9 |
| | T16-C | 212 | 804 | 843 | 1.05 | 0.068 | 19.3 |
| | Average | 209 | 800 | 844 | 1.05 | 0.066 | 19.0 |

## 2.4 Test Setup

All the tests were conducted with a 1,000 tons universal servo-controlled testing machine, and the general test setup is shown in Figure 3. A pair of attachments were connected to both ends of the H-sections through bolts. These attachments provided an eccentricity of about 100 mm along the minor axes of the H-sections for the applied loads to act upon. They also enabled the H-sections to rotate freely at both ends about the minor axes of the sections.

A total of twelve strain gauges were mounted onto the outer surfaces of the flanges of the H-sections at three cross-sections, namely, Sections A-A, B-B and C-C. At each section, four strain gauges were installed 10 mm away from the edges of the flanges. Displacement transducers DT1, DT2, DT3 and DT4 were used to measure lateral deflections of the H-sections at these three sections along the direction of the major axes of their cross-sections. It should be noted that any difference in the measurements between Transducers DT2 and DT3 would give a twisting of the H-sections along their longitudinal axes. Transducer DT5 was used to capture any lateral deflection of the H-section along the minor axes at Section B-B for a monitoring purpose while Transducer DT6 was used to measure axial deformations of the H-sections.

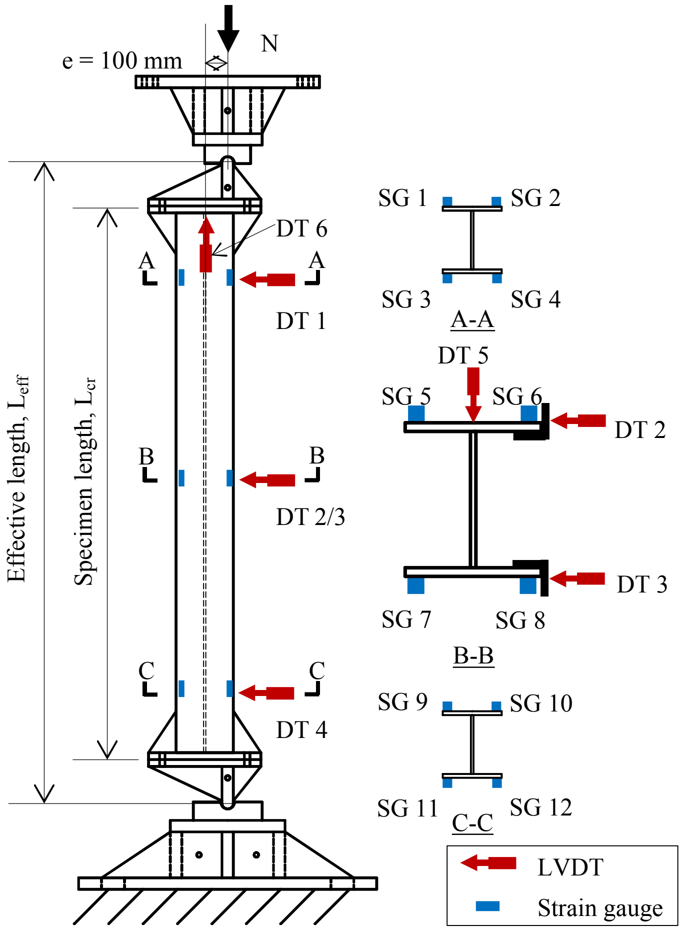


**Figure 3 Test setup for welded H-sections under eccentric loads**

## 2.5 Initial out-of-straightness

Before testing, the initial out-of-straightness of each H-section was measured. A steel wire was attached onto the surface of one flange of the H-section, and it ran through the centreline of the flange from Section A-A to Section C-C. Any deviation of the flange at the mid-height of the H-section was regarded as the initial out-of-straightness of this flange, $v_1$. Measurement was repeated on the other flange to obtain $v_2$ . The average value of $v_1$ and $v_2$ was considered to be the initial out-of-straightness, v , of the H-section, and these measurements for all H-sections are summarized in Table 4. Due to limitations of the measuring method, any value of measurement smaller than the radius of the steel wire, i.e. 0.25 mm, could not be recognized, and this situation is denoted with "---". Thus, it is shown that the absolute values of the measured out-of-straightness of all the H-sections are smaller than 1.0 mm, or 1/1000 of their effective lengths, $L_{eff}$. Thus, the magnitudes of these initial out-of-straightnesses would have very little effects on buckling behavior of the H-sections. In general, quality of the workmanship in fabricating these high strength Q690 steel welded H-sections was considered to be high, and readily achieved in modern fabrication shops.

**Table 4 Initial out-of-straightness at mid-height of welded H-sections**

| Test | $v_1$ (mm) | $v_2$ (mm) | $v$ (mm) | $L_{eff}$ (mm) | $\lvert v \rvert / L_{eff}$ ($\times 10^{-3}$) |
|---|---|---|---|---|---|
| EH1P | --- | +0.3 | +0.2 | 1992.0 | 0.1 |
| EH1Q | -0.5 | -0.5 | -0.5 | 2790.1 | 0.2 |
| EH2P | +0.2 | --- | +0.1 | 1993.3 | 0.1 |
| EH2Q | -0.5 | -0.5 | -0.5 | 2790.3 | 0.2 |
| E3HP | --- | --- | 0 | 1993.3 | 0.0 |
| E3HQ | -1.5 | -0.5 | -1.0 | 2791.6 | 0.4 |
| E4HP | -0.5 | -0.5 | -0.5 | 1990.5 | 0.3 |
| E4HQ | --- | --- | 0 | 2790.1 | 0.0 |

Notes:

a) "---" represents a value smaller than 0.25, and it may be taken to be 0.
b) $v = (v_1 + v_2) / 2$.
c) The signs of these values indicate the positions of the deviations.

### 2.6 Test procedure

In the initial stage of testing, a load was applied at a loading rate of 30 to 105 kN/min onto the H-sections, depending on their cross-sectional areas. Under this loading condition, the average stress rate for each H-section was kept to be smaller than 10 N/mm$^2$/min. This loading rate was maintained until 80% of the predicted failure load (or resistances) of each H-section was attained. Refer to Section 4 for details of the relevant design rules in predicting failure resistances of the H-sections. Then, a displacement control was adopted with a deformation rate of 0.5 mm/min. Under this displacement rate, the average strain rate for each H-section was smaller than 0.00025 / min., and hence, these tests should be regarded as static tests. In general, the test would be terminated after the applied load attained its maximum value, and dropped to 85% of the maximum value.

## 3 Test Results

All the H-sections were tested successfully, and experimental results of all these tests are presented in this section.

### 3.1 Failure modes and failure loads

All the H-sections failed in overall flexural buckling about the minor axes of their cross-sections as shown in Figure 4. There was also local plate buckling in the flange outstands of some of the H-sections, as shown in Figure 5. The failure loads, $N_{test}$ , of all the H-sections are summarized in Table 5. It should be noted that after testing, all the welded H-sections were inspected closely, and no welding fracture was found in any of the welded H-sections.

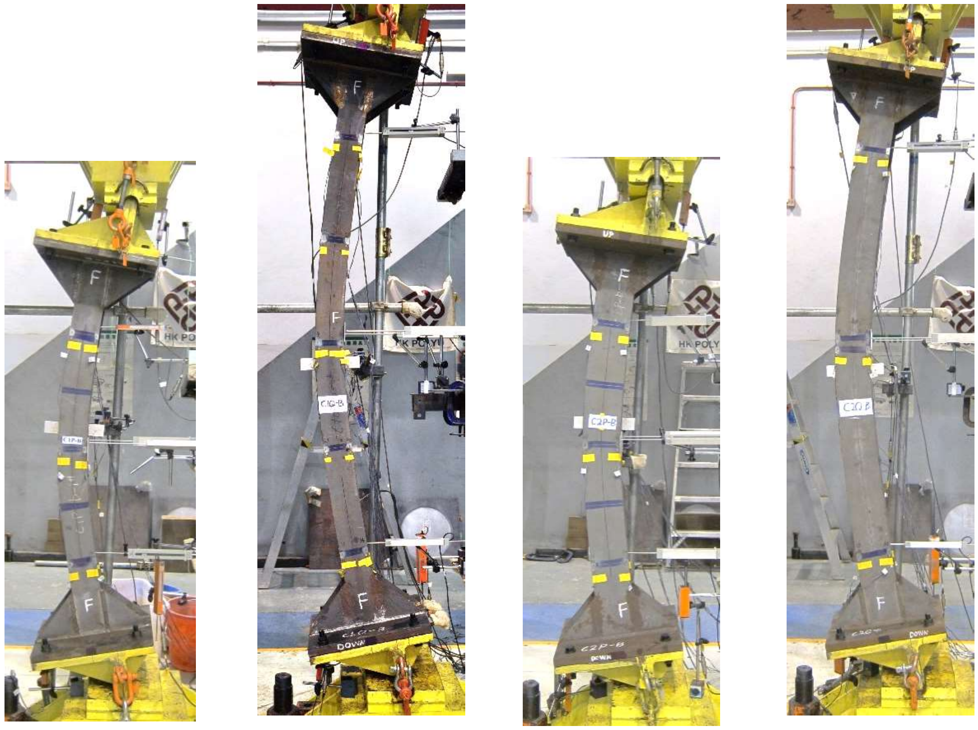

(a) Test EH1P (b) Test EH1Q (c) Test EH2P (d) Test EH2Q

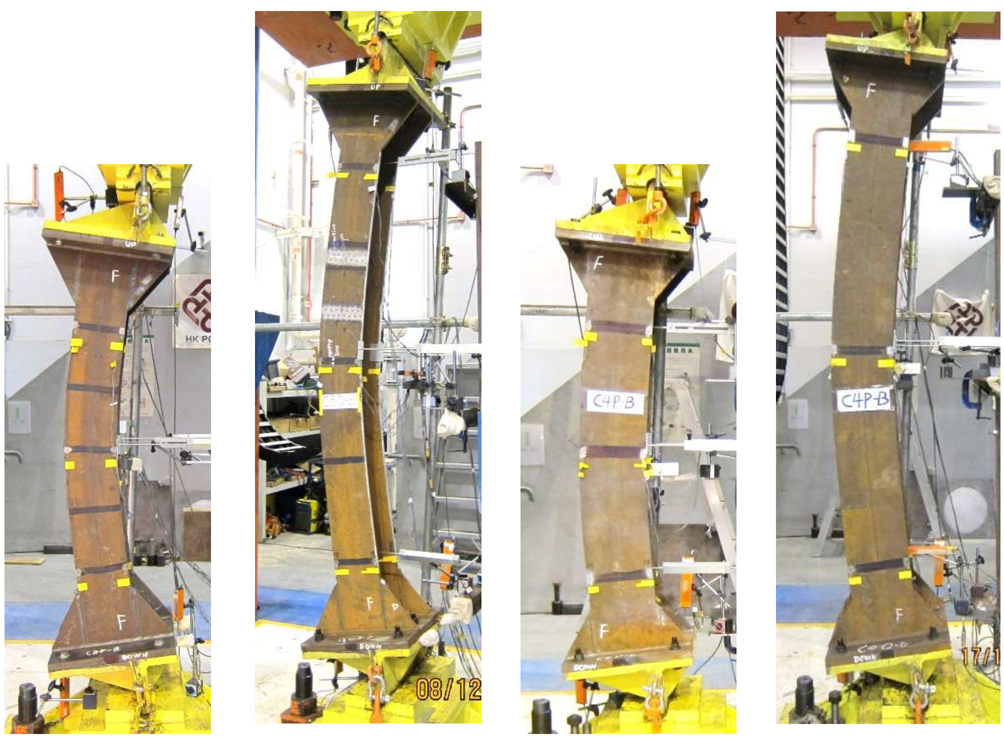


(e) Test EH3P (f) Test EH3Q (g) Test EH4P (h) Test EH4Q

**Figure 4 Overall flexural buckling of welded H-sections under eccentric loads**

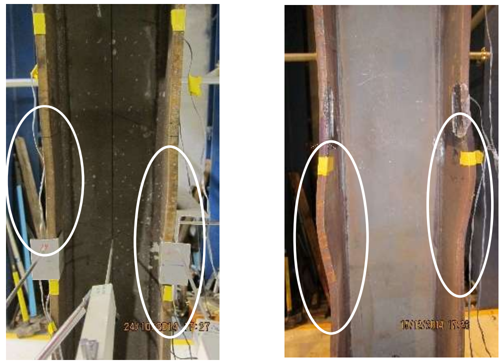

a) Test EH3P b) Test EH4P

**Figure 5 Local plate buckling in welded H-sections**

**Table 5 Test results of welded H-sections under combined compression and bending**

| Test | $N_{test}$ (kN) | Failure Mode | $\bar{\lambda}_z$ | $\lambda_z$ | Section Classification |
|---|---|---|---|---|---|
| EH1P | 328 | FB with LPP | 1.26 | 66 | 1 |
| EH1Q | 250 | FB | 1.77 | 92 | |
| EH2P | 527 | FB with LPP | 1.01 | 53 | 3 |
| EH2Q | 418 | FB | 1.42 | 74 | |
| EH3P | 1698 | FB with LPP | 0.77 | 39 | 2 |
| EH3Q | 1376 | FB with LPP | 1.08 | 55 | |
| EH4P | 2662 | FB with LPP | 0.62 | 32 | 3 |
| EH4Q | 2276 | FB with LPP | 0.87 | 44 | |

Note: "FB" stands for flexural buckling and "LPP" stands for local plate buckling.

## 3.2 Load-deformation relationships

For all welded H-sections, lateral deflections of the flanges at mid-height was recorded by Transducers DT2 and DT3. Hence, the average values of these two transducer readings were regarded as the lateral deflections, Δy, of the welded H-sections. The relationships between the applied load, N, and the lateral deflection, Δy, of all welded H-sections are shown in Figure 6. It should be noted that the maximum differences between these two transducer readings were found to be smaller than 0.2 mm throughout the testing, and hence, twisting of the H-sections at mid-height of the welded H-sections was considered to be insignificant in the present tests.

Moreover, axial deformations of the welded H-sections, Δx, were measured with Transducer DT6. The relationships between the applied load, N, and the axial deformation, Δx of all the welded H-sections are shown in Figure 7.

It is shown that both the lateral deflections, Δy, and the axial deformations, Δx, increase almost linearly with an increase of the applied load, N, up to failure in all tests. After the failure loads, $N_{test}$ , were attained, unloading took place gradually with further deformations in all the welded H-sections. In general, all of these load deformation relationships are considered to be similar to those slender columns of welded H-sections made of conventional steel materials.

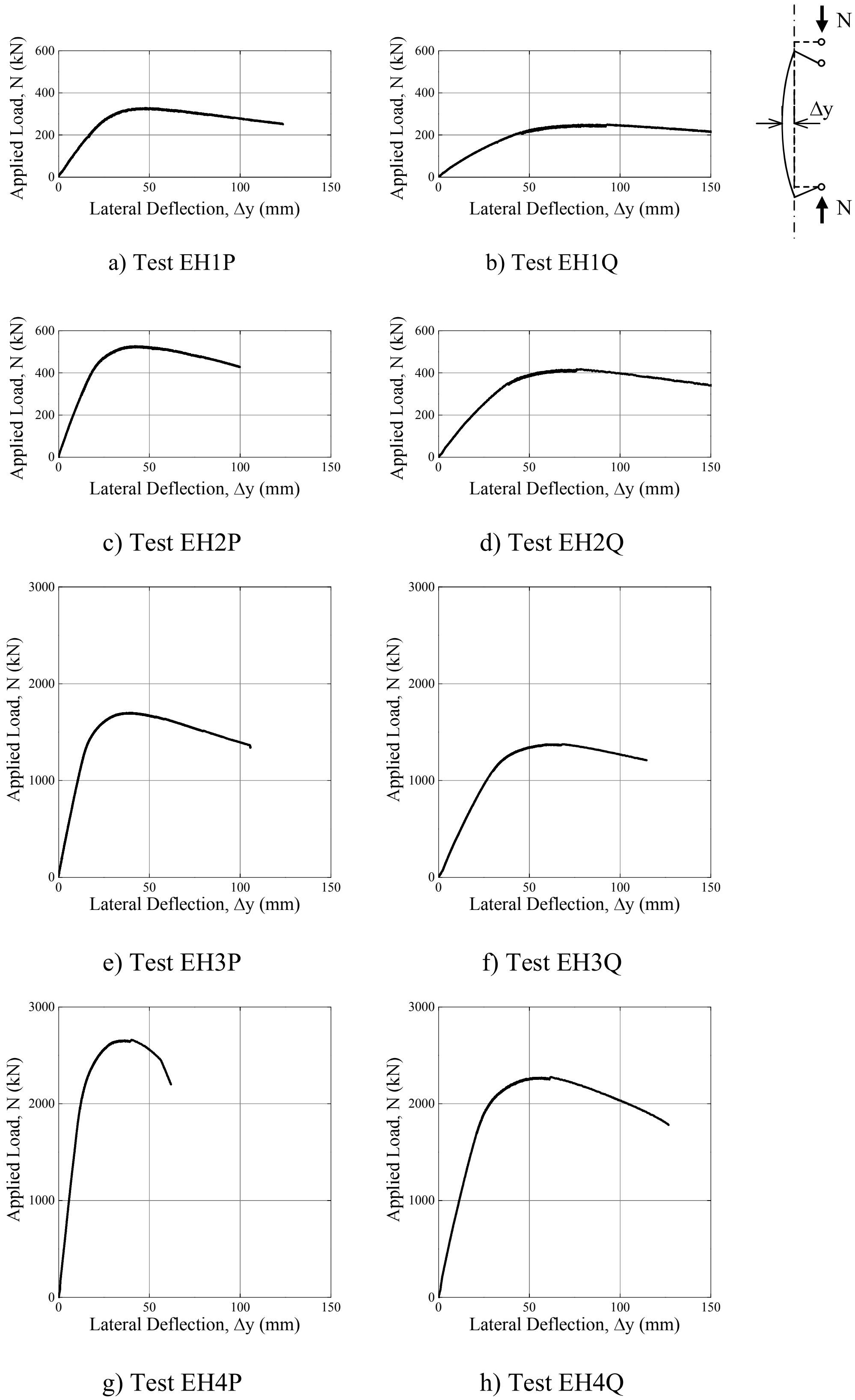


**Figure 6 Relationships between applied loads and lateral deflections for welded H-sections under combined compression and bending**

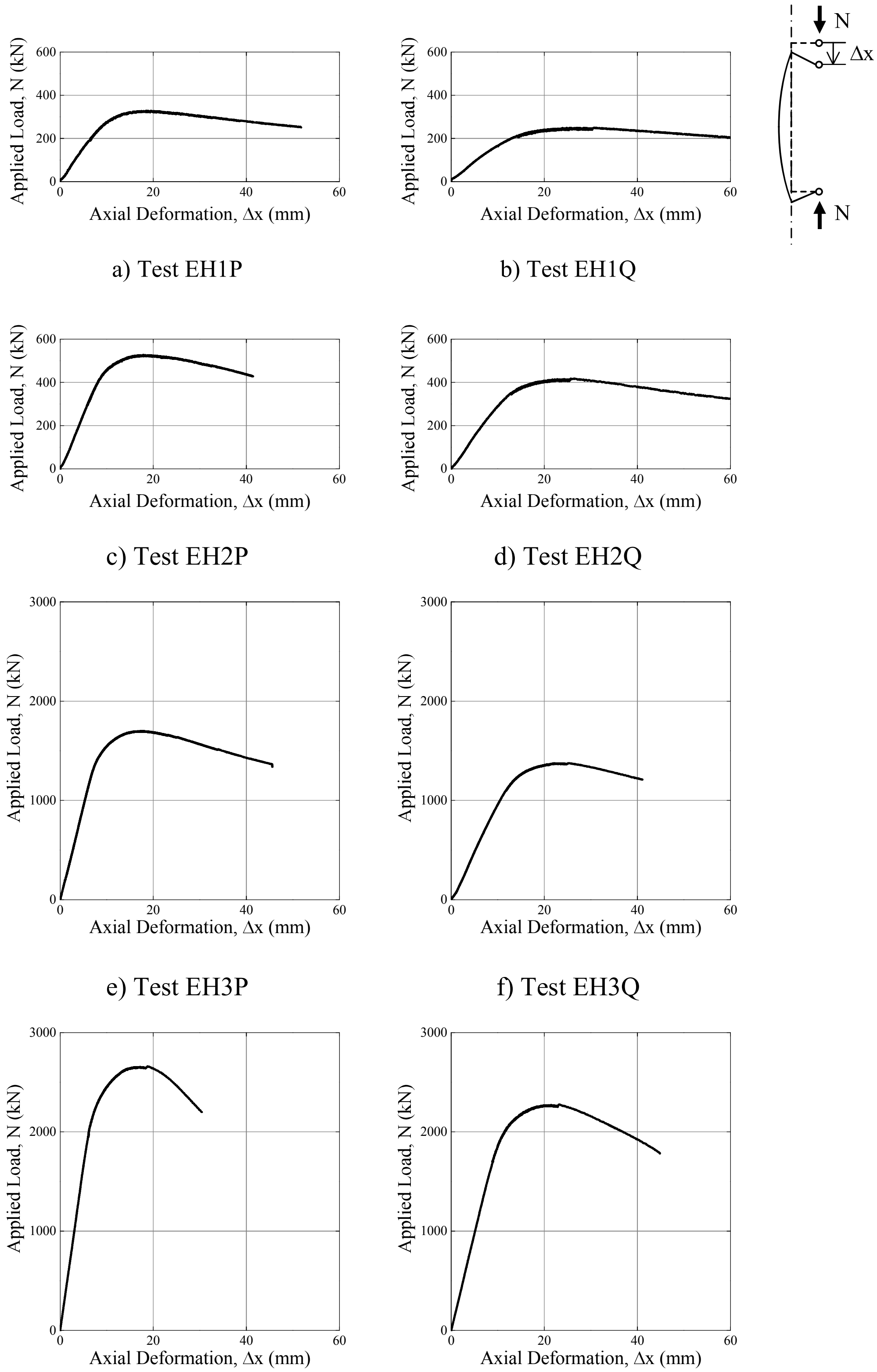


a) Test EH1P

b) Test EH1Q

c) Test EH2P

d) Test EH2Q

e) Test EH3P

f) Test EH3Q

g) Test EH4P

h) Test EH4Q

**Figure 7 Relationships between applied loads and axial deformations for welded H-sections under combined compression and bending**

### 3.3 Relationship between applied loads and axial strains

For each H-section, there were a total of twelve strain gauges mounted onto the outer surfaces of their two flanges, and these strain gauges were divided into a group of 4 strain gauges at three different cross-sections, namely Sections A-A, B-B and C-C. It is interesting to plot development of these axial strains measured at these three cross-sections during load application. Figure 8 plots relationships between the applied load, N, and the axial strains, $\varepsilon_x$ , at various cross-sections of Test EH3P for easy comparison. It should be noted that under the presence of combined compression and bending at mid-height of the welded H-section, i.e. Section B-B, measured resultant axial stresses from Strain Gauges SG 6 and 8 are found to be in compression while those from Strain Gauges SG 5 and 7 are in tension. As the applied load increases, the strain readings of these four strain gauges exceed the value of the yield strain, $\varepsilon_y$ , (or $f_y$ / E ). Hence, yielding occurs, leading the H-section to fail in an elastro-plastic manner.

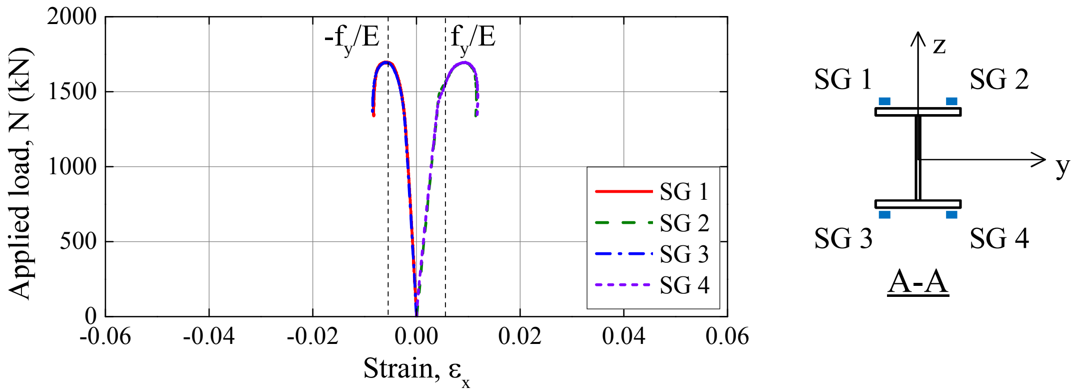


a) Section A-A

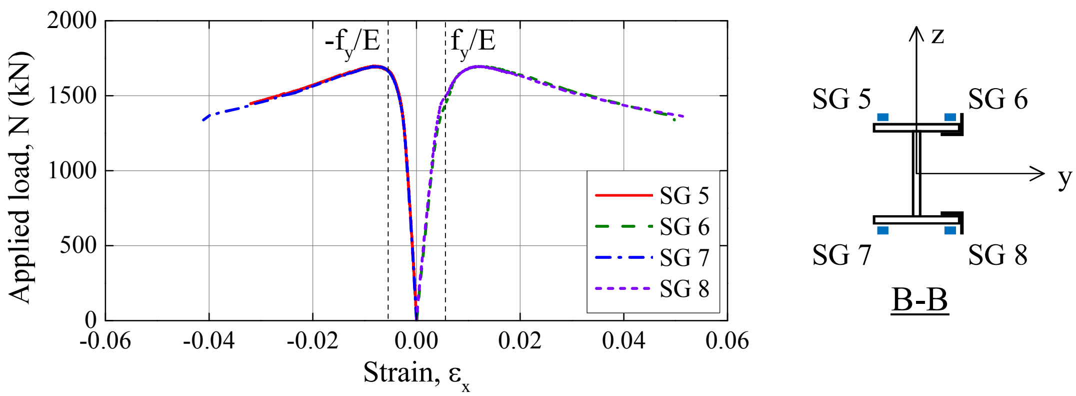


b) Section B-B

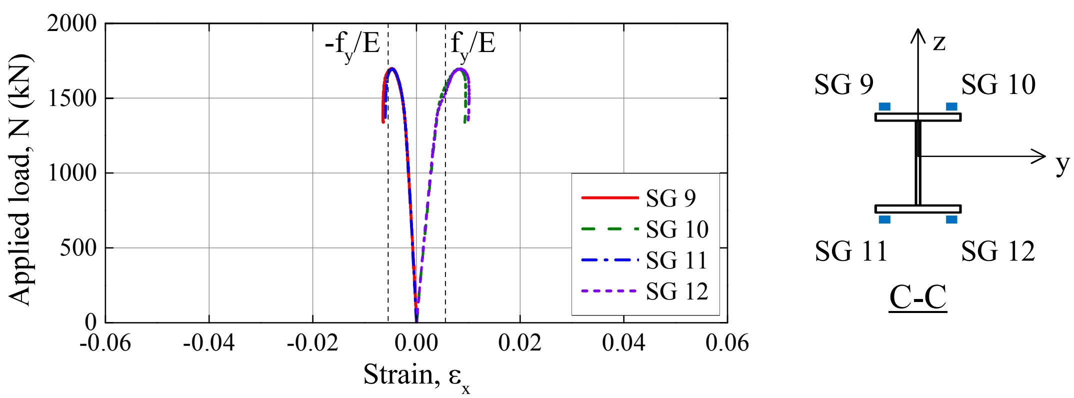


c) Section C-C

**Figure 8 Relationships between applied load and axial strains of welded H-sections – test EH3P**

## 3.4 Initial loading eccentricity

The initial loading eccentricities at Section A-A, $e_A$, and Section C-C, $e_C$, are defined as the eccentricities of the rotation centers at the H-section ends with respect to the line passing through the centerline of the flange at Sections A-A and C-C before loading respectively, as shown in Figure 9. The measured initial loading eccentricities, $e_A$ and $e_C$, for the welded H-sections in an elastic stage were obtained by using the applied load readings, and the corresponding strain readings and lateral deflections under the applied load at Sections A-A and C-C respectively. For Section A-A, the strain distribution of the whole cross-section was obtained using strain readings measured by Strain Gauges SG5, SG6, SG7 and SG 8. The stress distribution at this cross-section was then obtained by using the stress-strain curves obtained from the coupon tests, and hence, the corresponding internal moment under the applied load, $M_{A,SG}$ was computed accordingly. Consequently, the initial loading eccentricity at Section A-A, $e_A$ was readily obtained through equilibrium consideration as follows:

$$e_A = \frac{M_{A,SG}}{N} - d_A \tag{1}$$

where N is the applied load in the initial loading stage, $d_A$ is the corresponding lateral deflection at Section A-A under the applied load, N. The initial loading eccentricity at Section C-C, $e_C$ was obtained from a similar process. Table 6 summarizes the initial loading eccentricities of all the welded H-sections. The average value of the initial loading eccentricities of each welded H-section was employed to calculate the first order applied moment in subsequent analyses and calibration.

**Table 6 Loading Eccentricities of all the welded H-sections**

| Test | Section A-A $e_A$ (mm) | Section C-C $e_C$ (mm) | Average $(e_A+e_C)/2$ (mm) |
|---|---|---|---|
| EH1P | +101.5 | +101.4 | +101.5 |
| EH1Q | +96.4 | +95.8 | +96.1 |
| EH2P | +106.0 | +101.6 | +103.8 |
| EH2Q | +98.4 | +101.0 | +99.7 |
| E3HP | +100.1 | +96.2 | +98.2 |
| E3HQ | +101.9 | +102.9 | +102.4 |
| E4HP | +97.8 | +102.3 | +100.1 |
| E4HQ | +99.1 | +98.0 | +98.6 |

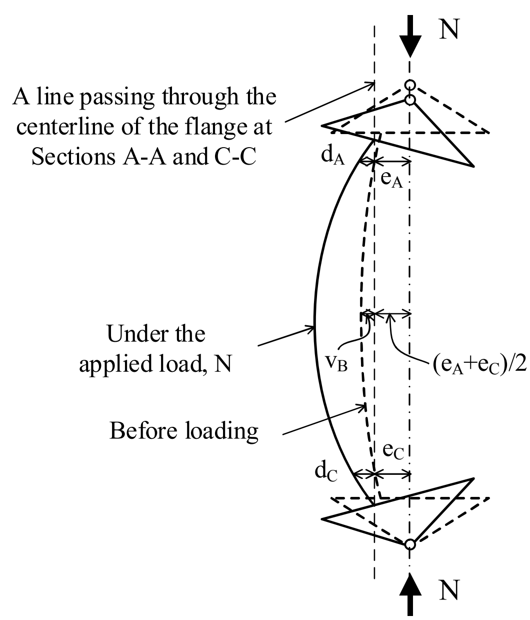


**Figure 9 Measurement of loading eccentricity**

# 4 Applicability of Design Rules

Applicability of design rules given in EN 1993-1-1, ANSI/AISC 360-16 and GB 50017-2003 for welded H-sections under combined compression and bending is assessed through calibration against the test results. In these design rules, effects of axial compression and bending moments are summed up linearly while non-linear effects of applied bending moments are accounted for by interaction factors. In general, two formulae should be satisfied, each of which corresponds to member buckling about a principal plane. However, as there was no applied moment about the major axes of the cross-sections of the H-sections, lateral-torsional buckling did not occur in the tests. Hence, the critical formula is the one corresponding to flexural buckling of the H-sections under bending about minor axes.

### 4.1.1 EN 1993-1-1

According to EN 1993-1-1, members which are subjected to combined compression and bending should satisfy:

$$\frac{N_{Ed}}{\frac{\chi_y N_{Rk}}{\gamma_{M1}}} + k_{yy}\frac{M_{y,Ed} + \Delta M_{y,Ed}}{\chi_{LT}\frac{M_{y,Rk}}{\gamma_{M1}}} + k_{yz}\frac{M_{z,Ed} + \Delta M_{z,Ed}}{\frac{M_{z,Rk}}{\gamma_{M1}}} \le 1 \qquad (2)$$

$$\frac{N_{Ed}}{\frac{\chi_z N_{Rk}}{\gamma_{M1}}} + k_{zy}\frac{M_{y,Ed} + \Delta M_{y,Ed}}{\chi_{LT}\frac{M_{y,Rk}}{\gamma_{M1}}} + k_{zz}\frac{M_{z,Ed} + \Delta M_{z,Ed}}{\frac{M_{z,Rk}}{\gamma_{M1}}} \le 1 \qquad (3)$$

where $N_{Ed}$, $M_{y,Ed}$, $M_{z,Ed}$ are the design values of the compression force and the moments about the major (y) and the minor (z) axes along the member, respectively;

$N_{Rk}$, $M_{y,Rk}$, $M_{z,Rk}$ are the characteristic values of resistances to compression force and the bending moments about the major (y) and the minor (z) axes, respectively;

$\Delta M_{y,Ed}$, $\Delta M_{z,Ed}$ are the moments due to the shift of the centroidal axes for class 4 sections;

$\chi_y$, $\chi_z$ are the reduction factors due to flexural buckling about the major (y) and the minor (z) axes, respectively;

$\chi_{LT}$ is the reduction factor due to lateral-torsional buckling;

$k_{yy}$, $k_{yz}$, $k_{zy}$, $k_{zz}$ are the interaction factors; and

$\gamma_{M1}$ is the partial factor for resistance of members to instability assessed by member checks.

The reduction factors $\chi_y$ and $\chi_z$ in the first terms in Equations (3) and (4) are determined by a suitable selection of flexural buckling curves. According to the complementary rules in EN 1993-1-12 for high strength Q690 steel welded H-sections, a curve "c" is recommended to calculate the flexural buckling resistances of the H-sections for buckling about the minor axes of the cross-sections. The interaction factors $k_{yy}$, $k_{yz}$, $k_{zy}$, and $k_{zz}$ in the second and the third terms may be obtained from two different approaches given in Annexes A and B respectively. It should be noted that the main difference between these two approaches is the way of presenting different structural effects. As Annex A emphasizes transparency, each structural effect is accounted for by an individual factor. However, Annex B works with simplicity and allows some structural effects to be combined into a global factor. Based on these two approaches, the design resistance $N_{EC3,c}$ for all the H-sections were calculated through iterations.

In the calculations, measured dimensions and mechanical properties as well as total initial geometrical imperfections were adopted. All the moment resistances of the H-sections are given by their plastic moduli even though Sections H2 and H4 are considered to be merely class 3 sections. Table 7 summarizes both the failure loads $N_{test}$ and the design resistances $N_{EC3,c}$ of the H-sections. It should be noted that:

- According to the approach given in Annex A, the values of $N_{test}$ / $N_{EC3,c}$ are found to range from 1.06 to 1.11 with an average value at 1.09.
- According to the approach given in Annex B, the values of $N_{test}$ / $N_{EC3,c}$ are found to range from 1.10 to 1.24 with an average value at 1.20.

Comparison between the test and the design resistances may be illustrated through plotting test values onto the graphs of normalized interaction curves according to the approaches in Annexes A and B for each of the four H-sections in Figure 10. As shown in the graphs, Annex B tends to give more conservative results when compared with Annex A.

It should be noted that in order to improve structural efficiency of the design rules, curve "a" is suggested to be used in the flexural buckling design of the welded H-sections to give the axial buckling resistances $N_{EC3,a}$ of the sections under combined compression and bending. The values of $N_{EC3,a}$ are also summarized in Table 7 for direct comparison with those of $N_{EC3,c}$ . It should be noted that:

- According to the approach given in Annex A, the values of $N_{test}$ / $N_{EC3,a}$ are found to range from 1.02 to 1.07 with an average value at 1.05.
- According to the approach given in Annex B, the values of $N_{test}$ / $N_{EC3,a}$ are found to range from 1.03 to 1.16 with an average value at 1.11.

Hence, by selecting a proper parameter in designing flexural resistances of the H-sections, the approaches in both Annexes A and B are shown to be significantly improved in giving conservative and yet efficient resistances for high strength Q690 steel welded H-sections under combined compression and bending about minor axes. The use of curve "a" in designing flexural resistances of welded H-sections is also supported by other researchers [9] [10] [12] as structural effects of residual stresses are proportionally less pronounced in these sections, when compared with those of conventional steel materials.

**Table 7 Calibration of EN 1993-1-1 for Q690 steel welded H-sections under combined compression and bending**

| Test | $N_{test}$ (kN) | $\lambda$ | $\bar{\lambda}$ | EN 1993-1-1: Annex A | | | | EN 1993-1-1: Annex B | | | |
|---|---|---|---|---|---|---|---|---|---|---|---|
| | | | | $N_{EC3,c}$ (kN) | $\frac{N_{test}}{N_{EC3,c}}$ | $N_{EC3,a}$ (kN) | $\frac{N_{test}}{N_{EC3,a}}$ | $N_{EC3,c}$ (kN) | $\frac{N_{test}}{N_{EC3,c}}$ | $N_{EC3,a}$ (kN) | $\frac{N_{test}}{N_{EC3,a}}$ |
| EH1P | 328 | 66 | 1.26 | 295 | 1.11 | 306 | 1.07 | 272 | 1.21 | 293 | 1.12 |
| EH1Q | 250 | 92 | 1.77 | 231 | 1.08 | 240 | 1.04 | 227 | 1.10 | 238 | 1.05 |
| EH2P | 527 | 53 | 1.01 | 477 | 1.10 | 495 | 1.07 | 425 | 1.24 | 461 | 1.14 |
| EH2Q | 418 | 74 | 1.42 | 386 | 1.08 | 402 | 1.04 | 362 | 1.15 | 393 | 1.06 |
| EH3P | 1698 | 39 | 0.77 | 1599 | 1.06 | 1666 | 1.02 | 1424 | 1.19 | 1523 | 1.12 |
| EH3Q | 1376 | 55 | 1.08 | 1250 | 1.10 | 1310 | 1.05 | 1129 | 1.22 | 1238 | 1.11 |
| EH4P | 2662 | 32 | 0.62 | 2481 | 1.07 | 2579 | 1.03 | 2185 | 1.22 | 2303 | 1.16 |
| EH4Q | 2276 | 44 | 0.87 | 2075 | 1.10 | 2179 | 1.04 | 1848 | 1.23 | 2018 | 1.13 |
| Average | --- | --- | --- | --- | 1.09 | --- | 1.05 | --- | 1.20 | --- | 1.11 |

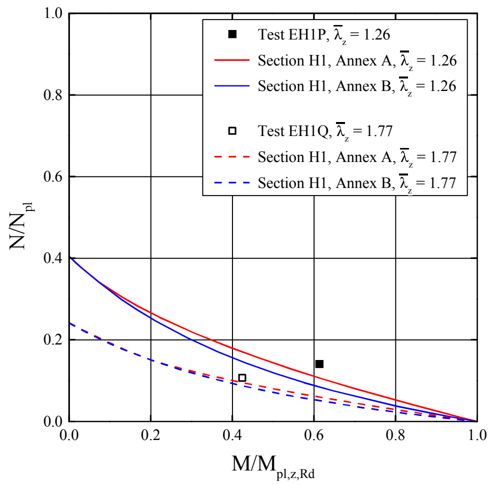


a) Section H1

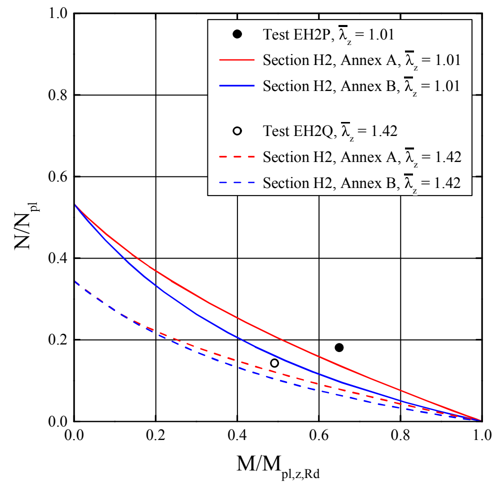


b) Section H2

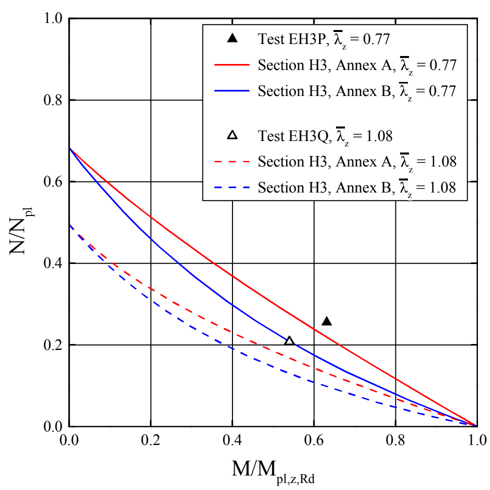


c) Section H3

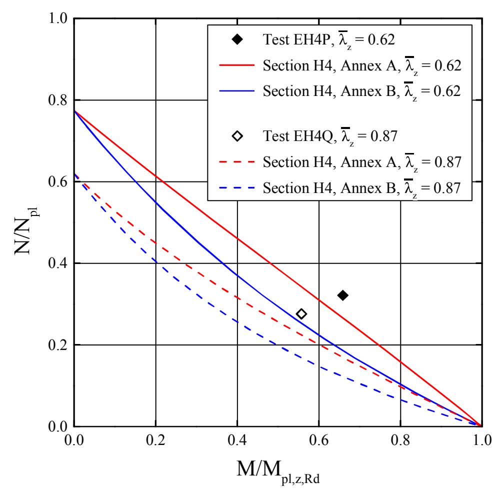


d)Section H4

**Figure 10 Normalized interaction curves to EN 1993-1-1**

### 4.1.2 ANSI/AISC 360-16

ANSI/AISC 360-16 is applicable to steel grades up to 690 N/mm$^2$ (ASTM A514 and A709 steel). For doubly and singly symmetric members subject to combined compression and bending, the following equations in ANSI/AISC 360-16 should be satisfied:

$$\text{When } \frac{P_r}{P_c} \geq 0.2 \qquad \frac{P_r}{P_c} + \frac{8}{9}\left(\frac{M_{rx}}{M_{cx}} + \frac{M_{ry}}{M_{cy}}\right) \leq 1.0 \tag{4}$$

$$\text{When } \frac{P_r}{P_c} < 0.2 \qquad \frac{P_r}{2P_c} + \left(\frac{M_{rx}}{M_{cx}} + \frac{M_{ry}}{M_{cy}}\right) \leq 1.0 \tag{5}$$

where $P_r$ is the design axial force;
$P_c$ is the axial buckling resistance;
$M_{rx}$, $M_{ry}$ are the design moments about the major (x) and the minor (y) axes respectively; and
$M_{cx}$, $M_{cy}$ are the moment resistances about the major (x) and the minor (y) axes respectively.

It should be noted that the design axial forces, $P_{r,ANSI}$ , for all the H-sections are calculated through iterations. Comparison between the test resistances $N_{test}$ and the design resistances $P_{r,ANSI}$ is shown in Table 8, and corresponding normalized interaction curves are plotted in Figure 11. It is found that the design rules in ANSI/AISC 360-16 tend to provide close but slightly un-conservative predictions to the failure loads of high strength Q690 steel welded H-sections under combined compression and bending about minor axes.

**Table 8 Calibration of ANSI/AISC 360-16 for Q690 steel welded H-sections under combined compression and bending**

| Test | $N_{test}$ (kN) | $\lambda$ | $\bar{\lambda}$ | ANSI/AISC 360-16 | |
|---|---|---|---|---|---|
| | | | | $P_{r,ANSI}$ (kN) | $\frac{N_{test}}{P_{r,ANSI}}$ |
| EH1P | 328 | 66 | 1.26 | 335 | 0.98 |
| EH1Q | 250 | 92 | 1.77 | 256 | 0.98 |
| EH2P | 527 | 53 | 1.01 | 515 | 1.02 |
| EH2Q | 418 | 74 | 1.42 | 426 | 0.98 |
| EH3P | 1698 | 39 | 0.77 | 1713 | 0.99 |
| EH3Q | 1376 | 55 | 1.08 | 1409 | 0.98 |
| EH4P | 2662 | 32 | 0.62 | 2449 | 1.09 |
| EH4Q | 2276 | 44 | 0.87 | 2182 | 1.04 |
| Average | --- | --- | --- | --- | 1.01 |

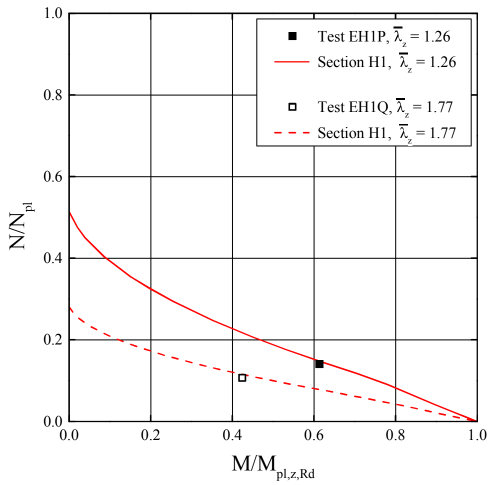


(a) Section H1

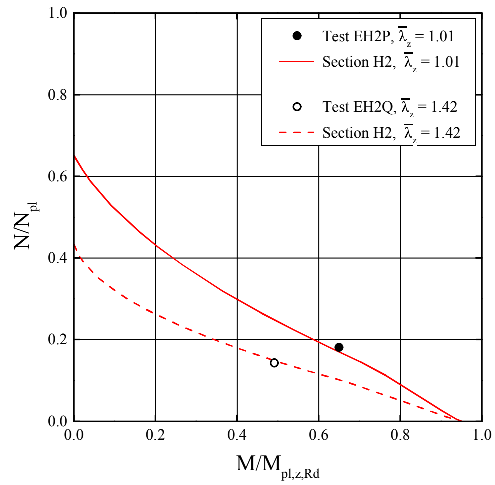


(b) Section H2

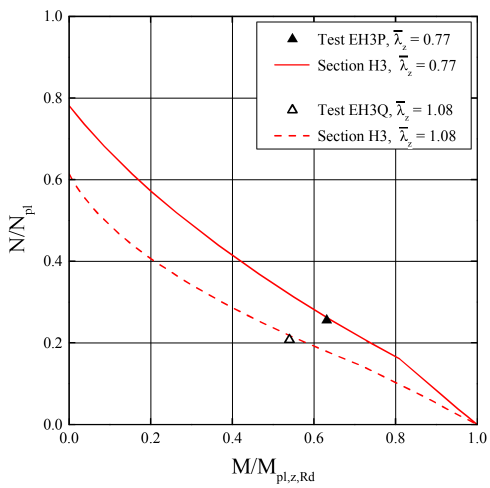


(c) Section H3

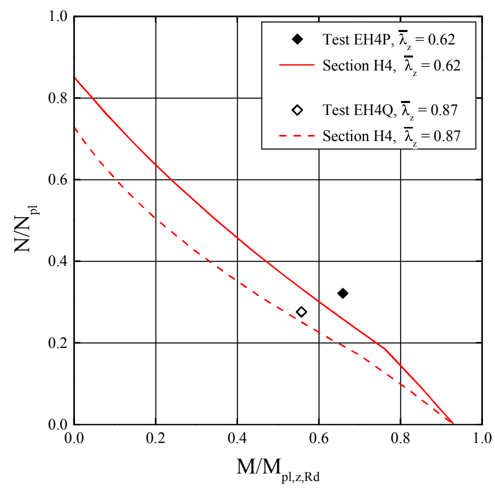


(d)Section H4

**Figure 11 Normalized interaction curves to ANSI/AISC 360-16**

### 4.1.3 GB 50017-2003

It should be noted that Q690 steel is beyond the scope of GB 50017-2003, and hence, it is necessary to verify its applicability to design Q690 steel materials. For members under combined compression and bending, the following equations in GB 50017-2003 should be satisfied:

$$\frac{N}{\varphi_x A}+\frac{\beta_{mx} M_x}{\gamma_x W_x\left(1-0.8\frac{N}{N'_{Ex}}\right)}+\eta\frac{\beta_{ty} M_y}{\varphi_{by} W_y}\le f \tag{6}$$

$$\frac{N}{\varphi_y A}+\eta\frac{\beta_{tx} M_x}{\varphi_{bx} W_x}+\frac{\beta_{my} M_y}{\gamma_y W_y\left(1-0.8\frac{N}{N'_{Ey}}\right)}\le f \tag{7}$$

where $N$ is the design value of the compression force;
$M_x$, $M_y$ are the design moments about the major (x) and the minor (y) axes, respectively;
$\varphi_x$, $\varphi_y$ are the reduction factors for flexural buckling about the major (x) and the minor (y) axes, respectively;
$\varphi_{bx}$ is the reduction factor for lateral-torsional buckling;
$\varphi_{by}$ $=1.0$ ;
$N'_{Ex}$ $=\pi^2 EA/\left(1.1\lambda_x^2\right)$;
$N'_{Ey}$ $=\pi^2 EA/\left(1.1\lambda_y^2\right)$;
$\lambda_x$, $\lambda_y$ are the slendernesses for flexural buckling about the major (x) and the minor (y) axes, respectively;
$A$ is the cross-sectional area;
$W_x$, $W_y$ are the elastic moduli about the major (x) and the minor (y) axes, respectively;
$\beta_{mx}$, $\beta_{my}$ are equivalent uniform in-plane moment factors about the major (x) and the minor (y) axes, respectively;
$\beta_{tx}$, $\beta_{ty}$ are equivalent uniform out-of-plane moment factors about the major (x) and the minor (y) axes, respectively;
$\gamma_x$, $\gamma_y$ are factors considering material plasticity when bending about the major (x) and the minor (y) axes, respectively;
$\eta$ =1.0 for members susceptible to torsional deformation;
=0.7 for members not susceptible to torsional deformation;
$f$ design yield strength of the steel material; and
$E$ is the Young's modulus of the steel material.

A curve "b" is recommended to calculate flexural resistances of welded H-sections made of Q420 steel, the highest steel grade incorporated in GB50017-2003. The corresponding design resistances $N_{GB,b}$ are adopted for calibration against the test results. In addition, a curve "a" is also permitted in the code, and the corresponding design resistances $N_{GB,a}$ are also adopted for calibration. It should be noted that both the design resistances $N_{GB,a}$ and $N_{GB,b}$ are obtained through iterations. Comparison between the failure loads and the design resistances are shown in Table 9 while normalized interaction curves are plotted in Figure 12. It is found that the test results are significantly higher than the design resistances obtained with either curve “b” or curve “a”.

**Table 9 Calibration of GB 50017-2003 for Q690 steel welded H-sections under combined compression and bending**

| Test | $N_{test}$ (kN) | $\lambda$ | $\bar{\lambda}$ | GB 50017-2003 | | | |
|---|---|---|---|---|---|---|---|
| | | | | $N_{GB,b}$ (kN) | $\frac{N_{test}}{N_{GB,b}}$ | $N_{GB,a}$ (kN) | $\frac{N_{test}}{N_{GB,a}}$ |
| EH1P | 328 | 66 | 1.26 | 268 | 1.23 | 275 | 1.19 |
| EH1Q | 250 | 92 | 1.77 | 218 | 1.15 | 223 | 1.12 |
| EH2P | 527 | 53 | 1.01 | 425 | 1.24 | 437 | 1.21 |
| EH2Q | 418 | 74 | 1.42 | 361 | 1.16 | 371 | 1.13 |
| EH3P | 1698 | 39 | 0.77 | 1380 | 1.23 | 1419 | 1.20 |
| EH3Q | 1376 | 55 | 1.08 | 1149 | 1.20 | 1191 | 1.16 |
| EH4P | 2662 | 32 | 0.62 | 2062 | 1.29 | 2110 | 1.26 |
| EH4Q | 2276 | 44 | 0.87 | 1860 | 1.22 | 1930 | 1.18 |
| Average | --- | --- | --- | --- | 1.21 | --- | 1.18 |

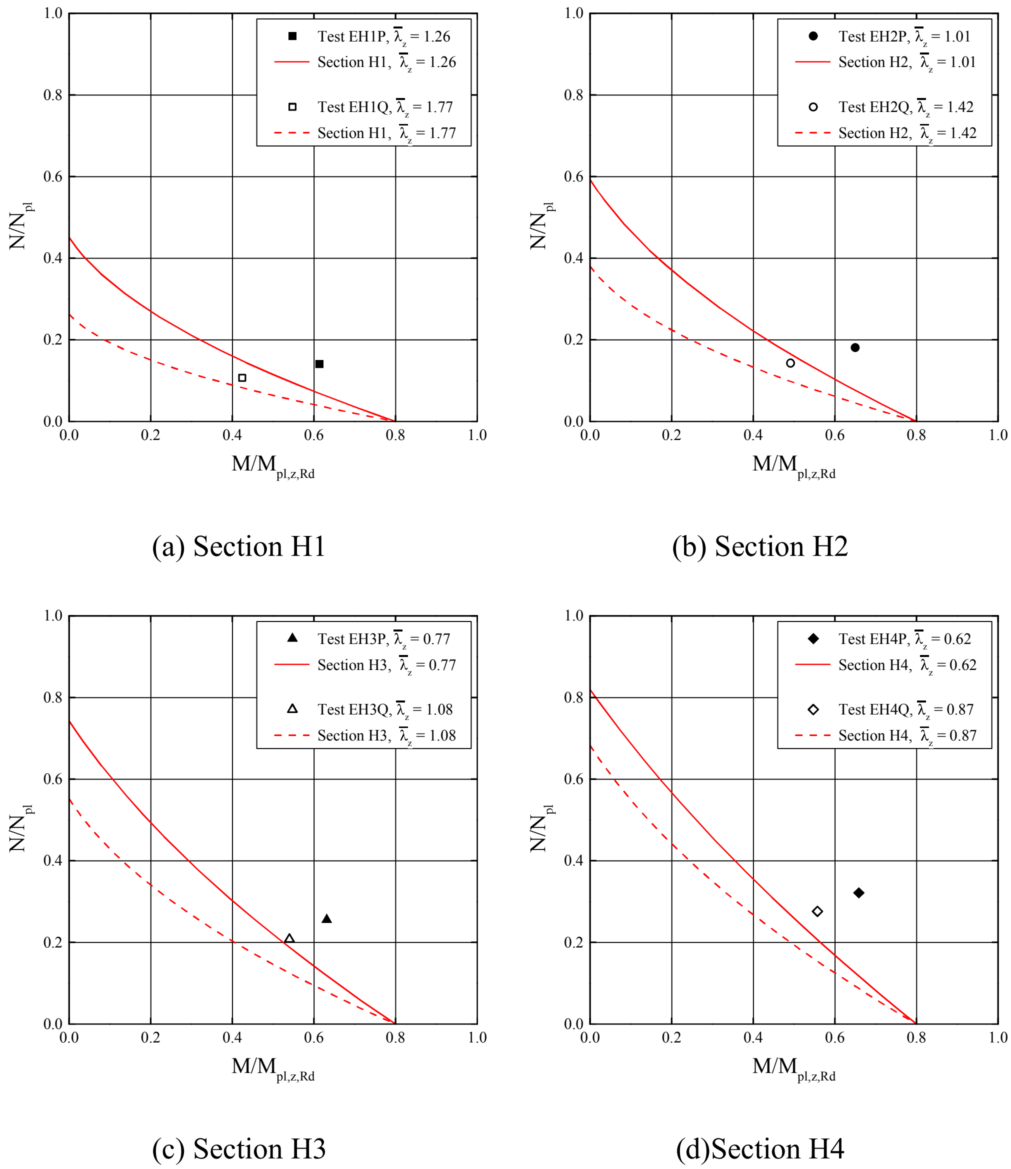


(a) Section H1

(b) Section H2

(c) Section H3

(d)Section H4

**Figure 12 Normalized interaction curves to GB 50017-2003**

## 5 Conclusions

A total of 8 high strength Q690 steel welded H-sections were tested successfully under combined compression and bending about minor axes. All of them failed in overall flexural buckling about the minor axes of their cross-sections with significant material yielding. In some cases, local plate buckling occurred in the flange outstands of the H-sections. No welding fracture was found in all the H-sections after testing. As expected, these high strength Q690 steel welded H-sections were demonstrated to behave in various ways similar to those of conventional strength steel welded H-sections. Hence, these tests may be regarded to be confirmatory tests to structural behavior of Q690 steel welded H-sections under combined compression and bending.

Applicability of design rules given in EN 1993-1-1, ANSI/AISC 360-16 and GB 50017-2003 to high strength Q690 steel welded H-sections under combined compression and bending about minor axes was examined through calibration against test results. It should be noted that the measured failure loads were compared with predicted resistances of these H-sections based on their measured geometrical and material properties according to various design rules. Among all these three sets of design rules, EN1993-1-1 was shown to be effective and efficient in predicting resistances for high strength steel Q690 steel welded H-sections under combined compression and bending with properly selected parameters. Hence, EN1993-1-1 should be readily adopted by design and construction engineers in designing these Q690 steel welded H-sections under combined compression and bending about minor axes.

## Acknowledgement

The authors are grateful to the financial support provided by the National Natural Science Foundation of China (Granted Project No. 51378378) and the Research Grant Council of the Government of Hong Kong SAR (Project No. PolyU 152194/15E). The project leading to the publication of this paper is also partially funded by the Research Committee and the Chinese National Engineering Research Centre for Steel Construction (Hong Kong Branch) of the Hong Kong Polytechnic University. The research studentships of the first three authors provided by the Tongji University and the Hong Kong Polytechnic University are acknowledged. Special thanks go to the Nanjing Iron and Steel Company Ltd. in Nanjing, the Zhongyi Steel Structure Co. Ltd. in Zhongshan and the Program Contractors Ltd. in Zhuhai. Thanks also go to the Hong Kong Constructional Metal Structures Association and the Macau Society of Metal Structures for their assistance in the fabrication of all the test specimens. All structural tests on high strength Q690 steel welded H-sections were carried out at the Structural Engineering Research Laboratory at the Hong Kong Polytechnic University, and supports from the technicians are gratefully acknowledged.

## Reference


[1] Y. J. Shi, “Recent Developments on High Performance Steel for Buildings,” *Adv. Struct. Eng.*, vol. 15, no. 9, pp. 1617–1622, 2012.

[2] B. Johansson and P. Collin, “Eurocode for high strength steel and applications in construction,” *Super-High Strength Steels*, 2005.

[3] C. Miki, K. Homma, and T. Tominaga, “High strength and high performance steels and their use in bridge structures,” *J. Constr. Steel Res.*, vol. 58, no. 1, pp. 3–20, 2002.

[4] R. Willms, “High strength steel for steel constructions,” *Nord. steel Constr. Conf.*, pp. 597–604, 2009.

[5] A. Azizinamini, K. Barth, R. Dexter, and C. Rubeiz, “High Performance Steel: Research Front—Historical Account of Research Activities,” *J. Bridg. Eng.*, vol. 9, no. 3, pp. 212–217, 2004.

[6] F. Schröter, “Trends of using high-strength steel for heavy steel structures,” *MA Giejowski, A. Kozowski, L. lczka, J. Zi{ó}ko Prog. Steel, Compos. Alum. Struct. S*, pp. 292–293, 2006.

[7] K. J. R. Rasmussen and G. J. Hancock, “Plate slenderness limits for high strength steel sections,” *J. Constr. Steel Res.*, vol. 23, no. 1–3, pp. 73–96, 1992.

[8] B. Yuan, “Local Buckling of High Strength Steel W-Shaped Sections,” McMaster University, 1997.

[9] K. J. R. Rasmussen and G. J. Hancock, “Tests of high strength steel columns,” *J. Constr. Steel Res.*, vol. 34, no. 1, pp. 27–52, 1995.

[10] T. J. Li, G. Q. Li, S. L. Chan, and Y. B. Wang, “Behavior of Q690 high-strength steel columns: Part 1: Experimental investigation,” *J. Constr. Steel Res.*, vol. 123, pp. 18–30, 2016.

[11] H. Y. Ban, G. Shi, Y. J. Shi, and M. A. Bradford, “Experimental investigation of the overall buckling behaviour of 960MPa high strength steel columns,” *J. Constr. Steel Res.*, vol. 88, pp. 256–266, 2013.

[12] G. Shi, H. Y. Ban, and F. S. K. Bijlaard, “Tests and numerical study of ultra-high strength steel columns with end restraints,” *J. Constr. Steel Res.*, vol. 70, pp. 236–247, 2012.

[13] Y. B. Wang, G. Q. Li, S. W. Chen, and F. F. Sun, “Experimental and numerical study on the behavior of axially compressed high strength steel box-columns,” *Eng. Struct.*, vol. 58, pp. 79–91, 2014.

[14] Y. B. Wang, G. Q. Li, S. W. Chen, and F. F. Sun, “Experimental and numerical study on the behavior of axially compressed high strength steel columns with H-section,” *Eng. Struct.*, vol. 43, pp. 149–159, 2012.

[15] H. Y. Ban, G. Shi, Y. J. Shi, and Y. Q. Wang, “Overall buckling behavior of 460MPa high strength steel columns: Experimental investigation and design method,” *J. Constr. Steel Res.*, vol. 74, pp. 140–150, 2012.

[16] F. Zhou, L. W. Tong, and Y. Y. Chen, “Experimental and numerical investigations of high strength steel welded h-section columns,” *Int. J. Steel Struct.*, vol. 13, no. 2, pp. 209–218, Jul. 2013.

[17] T. Usami and Y. Fukumoto, “Local and Overall Buckling of Welded Box Columns,” *J. Struct. Div.*, vol. 108, no. 3, pp. 525–542, 1982.

[18] G. Li, X. Yan, and S. Chen, “Experimental study on bearing capacity of welded H-section columns using Q460 high strength steel under bending and axial compression,” *J. Build. Struct.*, vol. 33, no. 12, pp. 31–37, 2012.

[19] G. Li, X. Yan, and S. Chen, “Experimental study on the ultimate bearing capacity of welded box-section columns using Q460 high strength steel in bending and axial compression,” *J. Build. Struct.*, vol. 45, no. 8, pp. 67–73, 2012.

[20] X. Yan, G. Li, and S. Chen, “Numerical analysis of the ultimate bearing capacity of welded box-section columns using Q460 high strength steel in bending and axial compression,” *Prog. Steel Build. Struct.*, vol. 15, no. 3, pp. 12–18, 2013.

[21] European Committee for Standardization, *BS EN 1993-1-1. Eurocode 3 - Design of steel structures - Part 1-1: General rules and rules for buildings*. Brussels, 2005.

[22] European Committee for Standardization, *BS EN 1993-1-12. Eurocode 3 - Design of steel structures - Part 1-12 : Additional rules for the extension of EN 1993 up to steel grades S 700*. Brussels, 2007.

[23] American Institute of Steel Construction, *ANSI/AISC 360-16. Specification for Structural Steel Buildings*. Chicago, 2016.

[24] Ministry of Construction of the People’s Republic of China, *GB 50017-2003. Code for Design of Steel Structures*. Beijing: China Architecture and Building Press, 2003.

[25] European Committee for Standardization, *BS EN ISO 6892-1:2009. Metallic materials - Tensile testing. Part 1: Method of test at ambient temperature*. Brussels, 2009.